



**University of
Zurich**^{UZH}

**Zurich Open Repository and
Archive**

University of Zurich
University Library
Strickhofstrasse 39
CH-8057 Zurich
www.zora.uzh.ch

Year: 2020

Observation of New Ξ_c^0 Baryons Decaying to $\Lambda_c^+ K^-$

LHCb Collaboration ; Bernet, R ; Müller, K ; Owen, P ; Serra, N ; Steinkamp, O ; et al

DOI: <https://doi.org/10.1103/PhysRevLett.124.222001>

Posted at the Zurich Open Repository and Archive, University of Zurich

ZORA URL: <https://doi.org/10.5167/uzh-196707>

Journal Article

Published Version



The following work is licensed under a Creative Commons: Attribution 4.0 International (CC BY 4.0) License.

Originally published at:

LHCb Collaboration; Bernet, R; Müller, K; Owen, P; Serra, N; Steinkamp, O; et al (2020). Observation of New Ξ_c^0 Baryons Decaying to $\Lambda_c^+ K^-$. Physical Review Letters, 124(22):222001.

DOI: <https://doi.org/10.1103/PhysRevLett.124.222001>

Observation of New Ξ_c^0 Baryons Decaying to $\Lambda_c^+ K^-$ R. Aaij *et al.*^{*}
(LHCb Collaboration) (Received 31 March 2020; revised manuscript received 4 May 2020; accepted 6 May 2020; published 4 June 2020)

The $\Lambda_c^+ K^-$ mass spectrum is studied with a data sample of pp collisions at a center-of-mass energy of 13 TeV corresponding to an integrated luminosity of 5.6 fb^{-1} collected by the LHCb experiment. Three Ξ_c^0 states are observed with a large significance and their masses and natural widths are measured to be $m[\Xi_c(2923)^0] = 2923.04 \pm 0.25 \pm 0.20 \pm 0.14 \text{ MeV}$, $\Gamma[\Xi_c(2923)^0] = 7.1 \pm 0.8 \pm 1.8 \text{ MeV}$, $m[\Xi_c(2939)^0] = 2938.55 \pm 0.21 \pm 0.17 \pm 0.14 \text{ MeV}$, $\Gamma[\Xi_c(2939)^0] = 10.2 \pm 0.8 \pm 1.1 \text{ MeV}$, $m[\Xi_c(2965)^0] = 2964.88 \pm 0.26 \pm 0.14 \pm 0.14 \text{ MeV}$, $\Gamma[\Xi_c(2965)^0] = 14.1 \pm 0.9 \pm 1.3 \text{ MeV}$, where the uncertainties are statistical, systematic, and due to the limited knowledge of the Λ_c^+ mass. The $\Xi_c(2923)^0$ and $\Xi_c(2939)^0$ baryons are new states. The $\Xi_c(2965)^0$ state is in the vicinity of the known $\Xi_c(2970)^0$ baryon; however, their masses and natural widths differ significantly.

DOI: [10.1103/PhysRevLett.124.222001](https://doi.org/10.1103/PhysRevLett.124.222001)

Singly charmed baryons are composed of a charm quark and two light quarks. Because of the large mass difference between the charm and the lighter quarks, these baryons provide an insight into the spectrum of states using symmetries described by the heavy quark effective theory [1,2]. Numerous theoretical predictions of the properties of heavy baryons, containing either a charm or a beauty quark, have been made in recent years [3–13]. In many of these models, the heavy quark interacts with a lighter diquark, which is treated as a single object. Other predictions are based on lattice QCD calculations [14].

In 2017, the LHCb Collaboration reported the observation of five new narrow Ω_c^0 baryons decaying to the $\Xi_c^+ K^-$ final state [15], four of which were later confirmed by the Belle Collaboration [16]. It is currently not understood why the natural widths of these resonances are small [17,18], although a similar trend has recently been observed in the excited Ω_b^- states decaying to $\Xi_b^0 K^-$ [19]. Investigating a different charmed mass spectrum could lead to a better understanding of this feature.

A natural extension to the $\Xi_c^+ K^-$ analysis is the study of the $\Lambda_c^+ K^-$ spectrum. The BABAR Collaboration was the first to observe a structure in the $\Lambda_c^+ K^-$ mass spectrum in $B^- \rightarrow K^- \Lambda_c^+ \bar{\Lambda}_c^-$ decays peaking at 2.93 GeV in 2007 [20]. However, it was not interpreted as a new state due to the absence of an amplitude analysis. Unless otherwise stated, charge-conjugate processes are implicitly included, and

natural units with $\hbar = c = 1$ are used throughout. Later that year, another analysis was published [21], looking at strongly interacting prompt decays of charm-strange baryons to several final states, one of which was $\Lambda_c^+ K^-$. No resonances were reported in the $\Lambda_c^+ K^-$ mass spectrum. The Belle Collaboration also reported the study of $B^- \rightarrow K^- \Lambda_c^+ \bar{\Lambda}_c^-$ decays [22]. A peaking structure was observed in the $\Lambda_c^+ K^-$ mass spectrum compatible with the results of Ref. [20] and interpreted as a new Ξ_c^0 baryon, dubbed $\Xi_c(2930)^0$. Similarly, evidence of the isospin partner $\Xi_c(2930)^+$ in $\bar{B}^0 \rightarrow \bar{K}^0 \Lambda_c^+ \bar{\Lambda}_c^-$ decays has been claimed [23].

This Letter presents a search for excited Ξ_c^0 baryons, hereafter referred to as Ξ_c^{*0} , in the $\Lambda_c^+ K^-$ spectrum in a mass region around the $\Xi_c(2930)^0$ state, with the Λ_c^+ baryons reconstructed in the $pK^-\pi^+$ final state. Defining $\Delta M \equiv m(\Lambda_c^+ K^-) - m(\Lambda_c^+) - m(K^-)$, the region considered is $\Delta M < 300 \text{ MeV}$. The data are collected in pp collisions with the LHCb detector at a center-of-mass energy of 13 TeV, corresponding to an integrated luminosity of 5.6 fb^{-1} .

The LHCb detector [24,25] is a single-arm forward spectrometer covering the pseudorapidity range $2 < \eta < 5$, designed for the study of particles containing b or c quarks. The detector elements that are particularly relevant to this analysis are a silicon-strip vertex detector surrounding the pp interaction region that allows c and b hadrons to be identified from their characteristically long flight distance; a tracking system that provides a measurement of the momentum of charged particles; and two ring-imaging Cherenkov detectors that are able to discriminate between different species of charged hadrons. The online event selection is performed by a trigger, which consists of a hardware stage, based on information from the calorimeter

^{*}Full author list given at the end of the article.

Published by the American Physical Society under the terms of the [Creative Commons Attribution 4.0 International license](https://creativecommons.org/licenses/by/4.0/). Further distribution of this work must maintain attribution to the author(s) and the published article's title, journal citation, and DOI. Funded by SCOAP³.

and muon systems, followed by a two-level software stage, which applies a full event reconstruction [26,27]. Simulated data samples are produced with the software packages described in Refs. [28–32] and are used to optimize the selection requirements, to quantify the invariant-mass resolution, and to model physics processes which may constitute peaking backgrounds in the analysis.

Candidate Λ_c^+ baryons are formed from the combination of three tracks of good quality which are inconsistent with originating from any primary proton-proton interaction vertex (PV) and have large transverse momentum (p_T). Particle identification (PID) requirements are imposed on all three tracks to suppress combinatorial background and misidentified charm-meson decays. The Λ_c^+ candidates are required to have $p_T > 2$ GeV and are constrained to originate from the associated PV by requiring a small χ_{IP}^2 , defined as the difference between the vertex fit χ^2 of the PV reconstructed with and without the candidate in question. The Λ_c^+ vertex must also be displaced from the associated PV such that the Λ_c^+ decay time is longer than 0.3 ps. A multivariate classifier based on a boosted decision tree (BDT) algorithm [33,34] implemented in the TMVA toolkit [35] is used to further improve the Λ_c^+ signal purity. The input variables given to the BDT are the χ^2 value of the Λ_c^+ decay-vertex fit, the Λ_c^+ flight distance between the production and decay vertex, the angle between the Λ_c^+ momentum vector and the line that joins the Λ_c^+ decay vertex with its associated PV, the χ_{IP}^2 and p_T of the Λ_c^+ candidate, and the χ_{IP}^2 and PID responses of the Λ_c^+ decay particles. The background sample used in the BDT training consists of the lower and upper sidebands of the $pK^-\pi^+$ invariant mass distribution, 2230–2250 and 2320–2340 MeV, respectively. The signal sample used is the Λ_c^+ sample in the data after subtracting the background by means of the sPlot technique [36], exploiting $m(pK^-\pi^+)$ as a discriminating variable. The training of the multivariate algorithm is carried out by using 20 000 candidates of the reconstructed Λ_c^+ candidates from the data recorded in 2016. The requirement on the BDT response is determined using 200 000 Λ_c^+ candidates by maximizing the figure of merit $S/\sqrt{S+B}$, where S is the Λ_c^+ signal yield extracted from a fit to the mass spectrum of Λ_c^+ candidates passing a given BDT requirement and B is the expected background yield. The value for B is extrapolated by scaling the background yield over the full mass range of the fit to a ± 15 MeV mass range around the Λ_c^+ peak.

Misidentified $D^+ \rightarrow K^-\pi^+\pi^+$, $D^+ \rightarrow K^+K^-\pi^+$, and $D_s^+ \rightarrow K^+K^-\pi^+$ background decays are observed after changing the mass hypothesis of the proton into a kaon or a pion. These background components are reduced by employing a tighter PID selection and requiring the invariant mass $m(K^+K^-)$ to differ by at least 10 MeV from the known $\phi(1020)$ mass [37]. Removing all candidates in mass windows around the $D_{(s)}^+$ mass distributions

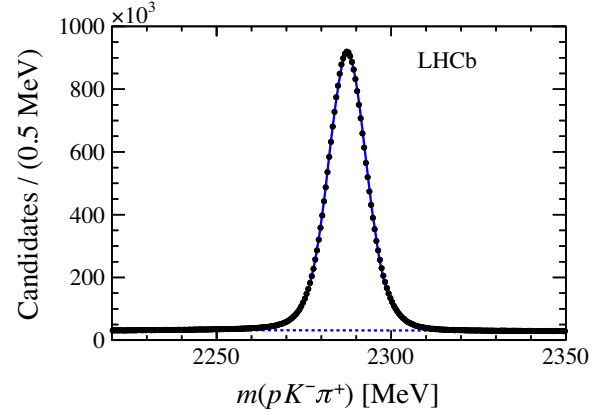


FIG. 1. Distribution of the reconstructed invariant mass $m(pK^-\pi^+)$ for 20% of the candidates in the Λ_c^+ sample passing the selection described in the text. The solid blue curve shows the result of the fit, and the dashed blue line indicates the background component of the fit.

would result in a large loss of signal efficiency and, therefore, is not implemented. However, it is checked that the results of the analysis are stable when these background components are removed fully. About 125 million Λ_c^+ signal decays are selected for further analysis with a purity of 93%. The invariant-mass distribution of 20% of the Λ_c^+ candidates satisfying these selection requirements is shown in Fig. 1.

The Ξ_c^{*0} candidates are formed from $\Lambda_c^+K^-$ combinations, where the Λ_c^+ candidate mass is required to be within 20 MeV of the known Λ_c^+ mass [37]. Each Λ_c^+ candidate is combined with a K^- candidate that is consistent with originating from the associated PV. The Λ_c^+ and K^- particles are fitted to a common vertex, which is required to be consistent with the associated PV.

The main contribution to the combinatorial background in the $\Lambda_c^+K^-$ mass spectrum is due to the large number of kaon candidates from the PV. The signal to background ratio is improved by optimising the PID criteria of the K^- candidates and the p_T requirement on the Ξ_c^{*0} candidates using the figure of merit $\epsilon/(\sqrt{B_p} + 5/2)$ [38]. Here, ϵ is the efficiency determined using simulated $\Xi_c(2930)^0 \rightarrow \Lambda_c^+K^-$ decays, and B_p is the number of $\Lambda_c^+K^-$ candidates in the mass region $260 < \Delta M < 290$ MeV, corresponding to the background expected in a mass window around the expected $\Xi_c(2930)^0$ signal, with width $\Gamma[\Xi_c(2930)^0] = 26 \pm 8$ MeV [37]. Based on the optimization above, the p_T of the Ξ_c^0 candidates is required to be larger than 7350 MeV, and the kaon PID is required to satisfy a tight criterion. The fraction of events with multiple candidates is found to be 0.88% in the entire ΔM range. All candidates are included in the analysis.

The resulting ΔM distribution of the signal candidates is shown in Fig. 2, where a fit to the data is superimposed. Three narrow structures are observed in the $\Lambda_c^+K^-$ candidate spectrum. These peaking structures are not seen in the

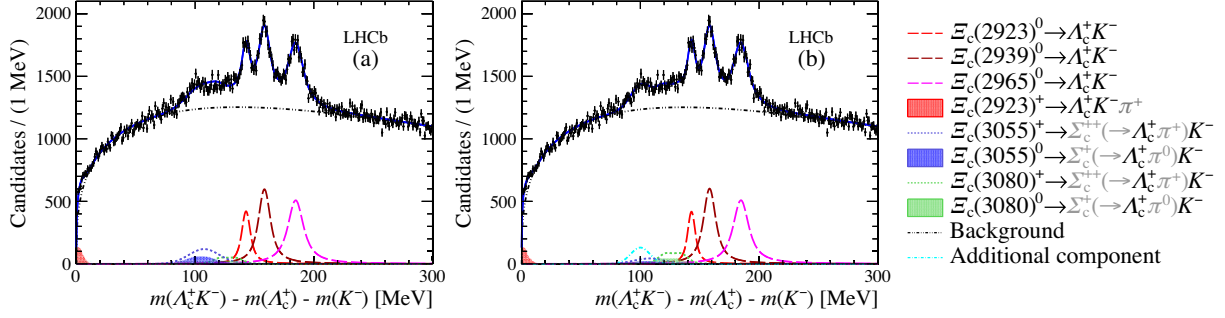


FIG. 2. Distributions of the reconstructed invariant-mass difference $\Delta M = m(\Lambda_c^+ K^-) - m(\Lambda_c^+) - m(K^-)$ for all candidates passing the selection requirements described in the text. The black symbols show the selected signal candidates. The result of a fit, described in the text, is overlaid (solid blue line). In (a), the reference fit is shown. (b) shows an alternative description to the data, where an additional Gaussian component given by the cyan dot-dashed line is added to the fit model around $\Delta M \simeq 100$ MeV. The missing child particles in the reconstruction are indicated in gray in the legend.

wrong-sign $\Lambda_c^+ K^+$ candidates or Λ_c^+ sideband distributions. The ΔM distribution also shows a broad structure to the left of the three narrow structures consistent with being partially reconstructed $\Xi_c(3055) \rightarrow \Sigma_c(2455)(\rightarrow \Lambda_c^+ \pi) K^-$ and $\Xi_c(3080) \rightarrow \Sigma_c(2455)(\rightarrow \Lambda_c^+ \pi) K^-$ decays, where the pion is not reconstructed.

An unbinned maximum-likelihood fit, henceforth denoted the reference fit, is performed to the ΔM distribution to measure the parameters of each peak. The background is modeled by an empirical function of the form $\Delta M^a \times \exp(-b \times \Delta M)$, where a and b vary freely. Each signal peak is described by an S -wave relativistic Breit-Wigner function convolved with a mass-resolution function. The experimental mass resolution is determined using simulated $\Xi_c^{*0} \rightarrow \Lambda_c^+ K^-$ decays at several Ξ_c^{*0} masses. In the ΔM interval where the three narrow peaks occur, the mass resolution varies between 1.7 and 2.2 MeV. Simulated data are also generated to determine the shape of partially reconstructed $\Xi_c(3055)$ and $\Xi_c(3080)$ decays. The shapes of these contributions are allowed to shift in ΔM by the uncertainties in the decay-product masses, where the shift is Gaussian constrained. From isospin symmetry, the yields of the $\Xi_c(3055)^+$ and $\Xi_c(3080)^+$ components are constrained to be twice as large as the corresponding $\Xi_c(3055)^0$ and $\Xi_c(3080)^0$ components. The fit model outlined so far does not accurately describe the data in the mass region close to the kinematic threshold, and, thus,

an additional component is considered. There are no known decays of $\Sigma_c(2455)(\rightarrow \Lambda_c^+ \pi) K^-$ or $\Sigma_c(2520)(\rightarrow \Lambda_c^+ \pi) K^-$ which could enter the sample as partially reconstructed components at $\Delta M \simeq 0$. It is observed that the missing component is consistent with being due to the partial reconstruction of the state that peaks around $\Delta M \simeq 140$ MeV when it decays directly to the $\Lambda_c^+ K^- \pi^+$ final state without any intermediate resonance. The shape of these partially reconstructed decays is taken from simulated samples generated using the RapidSim package [39], and the yield is a free parameter in the fit.

The ΔM distribution with the fit to the data superimposed is shown in Fig. 2(a). The goodness-of-fit value is $\chi^2/\text{ndof} = 301/(300 - 19) = 1.07$, where ndof is the number of degrees of freedom. Table I shows the results for the parameters of the signal peaks of the reference fit, hereafter named $\Xi_c(2923)^0$, $\Xi_c(2939)^0$, and $\Xi_c(2965)^0$.

To validate the presence of the signal components and test the stability of the fit parameters, several additional checks are performed. The data are fitted in samples according to the year of data taking and to different data-taking conditions depending on the LHCb magnet configuration. The $\Lambda_c^+ K^-$ sample and its charge conjugate are also studied separately. The results are consistent among all samples.

The data and the reference fit show the least compatibility in the region around $\Delta M \simeq 100$ MeV. This may be due to a mismodeling of the partially reconstructed distributions, but it could also be due to the presence of further new Ξ_c^{*0} baryon states. Figure 2(b) shows the ΔM distribution for the signal sample where an additional component, parametrized by an empirical Gaussian function, has been added to the reference fit. The fit has a goodness-of-fit value of $\chi^2/\text{ndof} = 278/(300 - 22) = 1.00$. As a cross-check, this structure is tested in subsamples of the dataset divided by data-taking year and showed an inconsistency in the scaling of the yield with respect to the integrated luminosity. Furthermore, the feed-down components are highly suppressed when this contribution

TABLE I. Peak positions in the invariant-mass difference distribution ΔM , natural widths Γ , signal yields, and local significances of the three mass peaks obtained from the fit to the $\Lambda_c^+ K^-$ mass spectrum, where the systematic uncertainties are statistical.

Peak of ΔM [MeV]	Γ [MeV]	Signal yields
142.91 ± 0.25	7.1 ± 0.8	5400 ± 400
158.45 ± 0.21	10.2 ± 0.8	10400 ± 600
184.75 ± 0.26	14.1 ± 0.9	11700 ± 600

TABLE II. Summary of the contributions to the systematic uncertainties on the resonance parameters. Absolute deviations from the nominal fit are quoted.

Source	$\Xi_c(2923)^0$		$\Xi_c(2939)^0$		$\Xi_c(2965)^0$	
	$m[\text{MeV}]$	$\Gamma[\text{MeV}]$	$m[\text{MeV}]$	$\Gamma[\text{MeV}]$	$m[\text{MeV}]$	$\Gamma[\text{MeV}]$
Alternative fit model	0.15	1.6	0.14	0.4	0.04	1.1
Resonance interferences	0.08	0.7	0.06	1.0	0.11	0.7
Momentum scale	0.04	...	0.05	...	0.06	...
Energy losses	0.04	...	0.04	...	0.04	...
Resolution calibration	...	0.6	...	0.2	...	0.3
Total	0.20	1.8	0.17	1.1	0.14	1.3

is included. More data are required to understand the cause of this additional structure. It is accounted for when calculating the systematic uncertainties.

Several sources of systematic uncertainty may affect the measured parameters. The fit model uncertainty is evaluated by replacing the background model by an alternative function, consisting of a combination of the wrong-sign $m(\Lambda_c^+ K^+)$ invariant-mass distribution shape and the shape obtained from candidates in the Λ_c^+ sideband. In addition, the choice of the relativistic Breit-Wigner model is changed by setting the values of the angular momentum L between the child particles to $L = 1, 2$ and separately varying the Blatt-Weisskopf factors [40] from 2 to 4 GeV^{-1} . Furthermore, the fit is adapted to include any partially reconstructed decays $\Xi_c^{**} \rightarrow \Sigma_c(2455/2520)(\rightarrow \Lambda_c^+ \pi) K^-$ that are found to not contribute significantly to the reference fit. Finally, deviations in fit parameters between the reference fit and the fit shown in Fig. 2(b) are included in the fit model uncertainty. The largest deviation from the reference fit is quoted as the systematic uncertainty for the fit model. Resonances with the same spin parity that are close in mass can interfere. An interference term is introduced between neighboring resonances, for one pair of resonances at a time. With the interference term, the line shape takes the form $A = |c_j \text{BW}_j + c_k \text{BW}_k e^{i\phi}|^2$, where j and k denote the two resonances, $\text{BW}_{j,k}$ are Breit-Wigner functions, and $c_{j,k}$ and ϕ are free real parameters. The largest difference between the reference fit and a fit where resonance interference is allowed is used as the systematic uncertainty. In addition, several other sources of systematic uncertainty affect only the mass measurement. These include the momentum-scale uncertainty, evaluated by shifting the momentum scale of charged

tracks by $\pm 0.03\%$ [41] in simulated decays, and the imperfect modeling of the energy loss in the detector material, resulting in a systematic uncertainty of 0.04 MeV [42]. Finally, a systematic uncertainty is attributed to the width measurement, to account for the fact that the simulation may not reproduce the absolute mass resolution perfectly. The corresponding systematic uncertainty is obtained by the change in the width when the value of the resolution, determined on simulated data, is varied by 10% [43]. The systematic uncertainties are summarized in Table II, and in Table III their measured masses and natural widths are summarized.

The observations described in this Letter and the lack of any $\Xi_c(2930)^0$ signal indicates that the broad bump observed in $B^- \rightarrow K^- \Lambda_c^+ \bar{\Lambda}_c^-$ decays [20,22] might be due to the overlap of two narrower states, such as the $\Xi_c(2923)^0$ and $\Xi_c(2939)^0$ baryons. The $\Xi_c(2965)^0$ baryon is in the vicinity of the known $\Xi_c(2970)^0$ baryon, which has been observed in different decay modes: $\Sigma_c(2455)^0 K_S^0$ [21], $\Xi_c'^+ \pi^-$ [44], and $\Xi_c(2645)^+ \pi^-$ [45]. Furthermore, the $\Xi_c(2965)^0$ resonance has a natural width and mass which differ significantly from those of the $\Xi_c(2970)^0$ baryon: $\Gamma[\Xi_c(2970)^0] = 28.1_{-4.0}^{+3.4} \text{ MeV}$ and $m[\Xi_c(2970)^0] = 2967.8_{-0.7}^{+0.9} \text{ MeV}$ [37]. Further studies are required to establish whether the $\Xi_c(2965)^0$ state is indeed a different baryon. The equal spacing rule [46,47] succeeded to predict the mass of the Ω baryon and holds for other flavor multiplets such as the sextet of the $J^P = 3/2^+$ charmed ground states:

$$m[\Omega_c(2770)^0] - m[\Xi_c(2645)^0] \simeq m[\Xi_c(2645)^0] - m[\Sigma_c(2520)^0] \simeq 125 \text{ MeV}.$$

 TABLE III. Summary of the parameters for the studied states, showing the measured ΔM values, the masses, and the natural widths, where the first uncertainty is statistical and the second uncertainty is systematic. For the mass measurement, the third uncertainty denotes the uncertainty on the known Λ_c^+ mass [37].

Resonance	Peak of ΔM [MeV]	Mass [MeV]	Γ [MeV]
$\Xi_c(2923)^0$	$142.91 \pm 0.25 \pm 0.20$	$2923.04 \pm 0.25 \pm 0.20 \pm 0.14$	$7.1 \pm 0.8 \pm 1.8$
$\Xi_c(2939)^0$	$158.45 \pm 0.21 \pm 0.17$	$2938.55 \pm 0.21 \pm 0.17 \pm 0.14$	$10.2 \pm 0.8 \pm 1.1$
$\Xi_c(2965)^0$	$184.75 \pm 0.26 \pm 0.14$	$2964.88 \pm 0.26 \pm 0.14 \pm 0.14$	$14.1 \pm 0.9 \pm 1.3$

It is noted that the rule also seems to hold for the $\Xi_c(2923)^0$, $\Xi_c(2939)^0$, and $\Xi_c(2965)^0$ baryons within a precision of a few MeV:

$$\begin{aligned} m[\Omega_c(3050)^0] - m[\Xi_c(2923)^0] \\ \simeq m[\Xi_c(2923)^0] - m[\Sigma_c(2800)^0] \simeq 125 \text{ MeV}, \\ m[\Omega_c(3065)^0] - m[\Xi_c(2939)^0] \simeq 125 \text{ MeV}, \\ m[\Omega_c(3090)^0] - m[\Xi_c(2965)^0] \simeq 125 \text{ MeV}. \end{aligned}$$

This pattern may indicate that the new states reported in this analysis are related to the excited Ω_c^0 baryons observed in the $\Xi_c^+ K^-$ spectrum. Measurements of spin parities will be crucial to confirm whether they belong to the same flavor multiplets.

In summary, pp collision data collected by the LHCb experiment at a center-of-mass energy of 13 TeV, corresponding to an integrated luminosity of 5.6 fb^{-1} , are used to search for excited Ξ_c^0 resonances in the $\Lambda_c^+ K^-$ mass spectrum. Three different Ξ_c^0 baryons, $\Xi_c(2923)^0$, $\Xi_c(2939)^0$, and $\Xi_c(2965)^0$, are unambiguously observed. The two baryons at lower mass are observed for the first time, while an investigation of additional final states is required to establish whether the $\Xi_c(2965)^0$ and $\Xi_c(2970)^0$ states are different baryons.

We express our gratitude to our colleagues in the CERN accelerator departments for the excellent performance of the LHC. We thank the technical and administrative staff at the LHCb institutes. We acknowledge support from CERN and from the national agencies: CAPES, CNPq, FAPERJ, and FINEP (Brazil); MOST and NSFC (China); CNRS/IN2P3 (France); BMBF, DFG, and MPG (Germany); INFN (Italy); NWO (Netherlands); MNiSW and NCN (Poland); MEN/IFA (Romania); MSHE (Russia); MinECo (Spain); SNSF and SER (Switzerland); NASU (Ukraine); STFC (United Kingdom); DOE NP and NSF (USA). We acknowledge the computing resources that are provided by CERN, IN2P3 (France), KIT and DESY (Germany), INFN (Italy), SURF (Netherlands), PIC (Spain), GridPP (United Kingdom), RRCKI and Yandex LLC (Russia), CSCS (Switzerland), IFIN-HH (Romania), CBPF (Brazil), PL-GRID (Poland), and OSC (USA). We are indebted to the communities behind the multiple open-source software packages on which we depend. Individual groups or members have received support from AvH Foundation (Germany); EPLANET, Marie Skłodowska-Curie Actions, and ERC (European Union); ANR, Labex P2IO, and OCEVU, and Région Auvergne-Rhône-Alpes (France); Key Research Program of Frontier Sciences of CAS, CAS PIFI, and the Thousand Talents Program (China); RFBR, RSF, and Yandex LLC (Russia); GVA, XuntaGal, and GENCAT (Spain); the Royal Society and the Leverhulme Trust (United Kingdom).

- [1] A. G. Grozin, Introduction to the heavy quark effective theory. Part 1, [arXiv:hep-ph/9908366](https://arxiv.org/abs/hep-ph/9908366).
- [2] T. Mannel, Effective theory for heavy quarks, *Lect. Notes Phys.* **479**, 387 (1997).
- [3] D. Ebert, R. N. Faustov, and V. O. Galkin, Masses of excited heavy baryons in the relativistic quark-diquark model, *Phys. Lett. B* **659**, 612 (2008).
- [4] W. Roberts and M. Pervin, Heavy baryons in a quark model, *Int. J. Mod. Phys. A* **23**, 2817 (2008).
- [5] H. Garcilazo, J. Vijande, and A. Valcarce, Faddeev study of heavy baryon spectroscopy, *J. Phys. G* **34**, 961 (2007).
- [6] S. Migura, D. Merten, B. Metsch, and H.-R. Petry, Charmed baryons in a relativistic quark model, *Eur. Phys. J. A* **28**, 41 (2006).
- [7] D. Ebert, R. N. Faustov, and V. O. Galkin, Spectroscopy and Regge trajectories of heavy baryons in the relativistic quark-diquark picture, *Phys. Rev. D* **84**, 014025 (2011).
- [8] A. Valcarce, H. Garcilazo, and J. Vijande, Towards an understanding of heavy baryon spectroscopy, *Eur. Phys. J. A* **37**, 217 (2008).
- [9] Z. Shah, K. Thakkar, A. K. Rai, and P. C. Vinodkumar, Mass spectra and Regge trajectories of Λ_c^+ , Σ_c^0 , Ξ_c^0 and Ω_c^0 baryons, *Chin. Phys. C* **40**, 123102 (2016).
- [10] J. Vijande, A. Valcarce, T. F. Carames, and H. Garcilazo, Heavy hadron spectroscopy: A quark model perspective, *Int. J. Mod. Phys. E* **22**, 1330011 (2013).
- [11] T. Yoshida, E. Hiyama, A. Hosaka, M. Oka, and K. Sadato, Spectrum of heavy baryons in the quark model, *Phys. Rev. D* **92**, 114029 (2015).
- [12] H.-X. Chen, W. Chen, Q. Mao, A. Hosaka, X. Liu, and S.-L. Zhu, P-wave charmed baryons from QCD sum rules, *Phys. Rev. D* **91**, 054034 (2015).
- [13] H.-X. Chen, Q. Mao, A. Hosaka, X. Liu, and S.-L. Zhu, D-wave charmed and bottomed baryons from QCD sum rules, *Phys. Rev. D* **94**, 114016 (2016).
- [14] M. Padmanath, R. G. Edwards, N. Mathur, and M. Peardon, Excited-state spectroscopy of singly, doubly and triply-charmed baryons from lattice QCD, in *Proceedings of the 6th International Workshop on Charm Physics (Charm 2013): Manchester, UK* (2013).
- [15] R. Aaij *et al.* (LHCb Collaboration), Observation of Five New Narrow Ω_c^0 States Decaying to $\Xi_c^+ K^-$, *Phys. Rev. Lett.* **118**, 182001 (2017).
- [16] J. Yelton *et al.* (Belle Collaboration), Observation of excited Ω_c charmed baryons in e^+e^- collisions, *Phys. Rev. D* **97**, 051102 (2018).
- [17] G. Chiladze and A. F. Falk, Phenomenology of new baryons with charm and strangeness, *Phys. Rev. D* **56**, R6738 (1997).
- [18] M. Karliner and J. L. Rosner, Very narrow excited Ω_c baryons, *Phys. Rev. D* **95**, 114012 (2017).
- [19] R. Aaij *et al.* (LHCb Collaboration), First Observation of Excited Ω_b^- States, *Phys. Rev. Lett.* **124**, 082002 (2020).
- [20] B. Aubert *et al.* (BABAR Collaboration), Study of $\bar{B} \rightarrow \Xi_c^- \bar{\Lambda}_c^+$ and $\bar{B} \rightarrow \Lambda_c^+ \bar{\Lambda}_c^- \bar{K}$ decays at BABAR, *Phys. Rev. D* **77**, 031101 (2008).
- [21] B. Aubert *et al.* (BABAR Collaboration), Study of excited charm-strange baryons with evidence for new baryons $\Xi_c(3055)^+$ and $\Xi_c(3123)^+$, *Phys. Rev. D* **77**, 012002 (2008).

- [22] Y. B. Li *et al.* (Belle Collaboration), Observation of $\Xi_c(2930)^0$ and updated measurement of $B^- \rightarrow K^- \Lambda_c^+ \bar{\Lambda}_c^-$ at Belle, *Eur. Phys. J. C* **78**, 252 (2018).
- [23] Y. B. Li *et al.* (Belle Collaboration), Evidence of a structure in $\bar{K}^0 \Lambda_c^+$ consistent with a charged $\Xi_c(2930)^+$, and updated measurement of $\bar{B}^0 \rightarrow \bar{K}^0 \Lambda_c^+ \bar{\Lambda}_c^-$ at Belle, *Eur. Phys. J. C* **78**, 928 (2018).
- [24] A. A. Alves, Jr. *et al.* (LHCb Collaboration), The LHCb detector at the LHC, *J. Instrum.* **3**, S08005 (2008).
- [25] R. Aaij *et al.* (LHCb Collaboration), LHCb detector performance, *Int. J. Mod. Phys. A* **30**, 1530022 (2015).
- [26] R. Aaij *et al.*, The LHCb trigger and its performance in 2011, *J. Instrum.* **8**, P04022 (2013).
- [27] R. Aaij *et al.*, Tesla: An application for real-time data analysis in high energy physics, *Comput. Phys. Commun.* **208**, 35 (2016).
- [28] T. Sjöstrand, S. Mrenna, and P. Skands, A brief introduction to PYTHIA 8.1, *Comput. Phys. Commun.* **178**, 852 (2008).
- [29] I. Belyaev *et al.*, Handling of the generation of primary events in Gauss, the LHCb simulation framework, *J. Phys. Conf. Ser.* **331**, 032047 (2011).
- [30] D. J. Lange, The EvtGen particle decay simulation package, *Nucl. Instrum. Methods Phys. Res., Sect. A* **462**, 152 (2001).
- [31] J. Allison *et al.* (Geant4 Collaboration), Geant4 developments and applications, *IEEE Trans. Nucl. Sci.* **53**, 270 (2006).
- [32] M. Clemencic, G. Corti, S. Easo, C. R. Jones, S. Miglioranza, M. Pappagallo, and P. Robbe, The LHCb simulation application, Gauss: Design, evolution and experience, *J. Phys. Conf. Ser.* **331**, 032023 (2011).
- [33] L. Breiman, J. H. Friedman, R. A. Olshen, and C. J. Stone, *Classification and Regression Trees* (Wadsworth International Group, Belmont, CA, 1984).
- [34] Y. Freund and R. E. Schapire, A decision-theoretic generalization of on-line learning and an application to boosting, *J. Comput. Syst. Sci.* **55**, 119 (1997).
- [35] H. Voss, A. Hoecker, J. Stelzer, and F. Tegenfeldt, TMVA—The Toolkit for Multivariate Data Analysis with ROOT, *Proc. Sci. ACAT2007* (**2007**) 040; A. Hoecker *et al.*, TMVA 4—Toolkit for Multivariate Data Analysis with ROOT. Users Guide, [arXiv:physics/0703039](https://arxiv.org/abs/physics/0703039).
- [36] M. Pivk and F. R. Le Diberder, sPlot: A statistical tool to unfold data distributions, *Nucl. Instrum. Methods Phys. Res., Sect. A* **555**, 356 (2005).
- [37] M. Tanabashi *et al.* (Particle Data Group), Review of particle physics, *Phys. Rev. D* **98**, 030001 (2018), and 2019 update.
- [38] G. Punzi, Sensitivity of searches for new signals and its optimization, eConf **C030908**, MODT002 (2003).
- [39] G. A. Cowan, D. C. Craik, and M. D. Needham, RapidSim: An application for the fast simulation of heavy-quark hadron decays, *Comput. Phys. Commun.* **214**, 239 (2017).
- [40] J. M. Blatt and V. F. Weisskopf, *Theoretical Nuclear Physics* (Springer, New York, 1952).
- [41] R. Aaij *et al.* (LHCb Collaboration), Precision measurement of D meson mass differences, *J. High Energy Phys.* **06** (2013) 065.
- [42] R. Aaij *et al.* (LHCb Collaboration), Prompt K_S^0 production in pp collisions at $\sqrt{s} = 0.9$ TeV, *Phys. Lett. B* **693**, 69 (2010).
- [43] R. Aaij *et al.* (LHCb Collaboration), Precision Measurement of the Mass and Lifetime of the Ξ_b^- Baryon, *Phys. Rev. Lett.* **113**, 242002 (2014).
- [44] J. Yelton *et al.* (Belle Collaboration), Study of excited Ξ_c states decaying into Ξ_c^0 and Ξ_c^+ baryons, *Phys. Rev. D* **94**, 052011 (2016).
- [45] T. Lesiak *et al.* (Belle Collaboration), Measurement of masses of the $\Xi_c(2645)$ and $\Xi_c(2815)$ baryons and observation of $\Xi_c(2980) \rightarrow \Xi_c(2645)\pi$, *Phys. Lett. B* **665**, 9 (2008).
- [46] M. Gell-Mann, Symmetries of baryons and mesons, *Phys. Rev.* **125**, 1067 (1962).
- [47] S. Okubo, Note on unitary symmetry in strong interactions, *Prog. Theor. Phys.* **27**, 949 (1962).

R. Aaij,³¹ C. Abellán Beteta,⁴⁹ T. Ackernley,⁵⁹ B. Adeva,⁴⁵ M. Adinolfi,⁵³ H. Afsharnia,⁹ C. A. Aidala,⁸¹ S. Aiola,²⁵ Z. Ajaltouni,⁹ S. Akar,⁶⁶ J. Albrecht,¹⁴ F. Alessio,⁴⁷ M. Alexander,⁵⁸ A. Alfonso Albero,⁴⁴ G. Alkhazov,³⁷ P. Alvarez Cartelle,⁶⁰ A. A. Alves Jr.,⁴⁵ S. Amato,² Y. Amhis,¹¹ L. An,²¹ L. Anderlini,²¹ G. Andreassi,⁴⁸ M. Andreotti,²⁰ F. Archilli,¹⁶ A. Artamonov,⁴³ M. Artuso,⁶⁷ K. Arzymatov,⁴¹ E. Aslanides,¹⁰ M. Atzeni,⁴⁹ B. Audurier,¹¹ S. Bachmann,¹⁶ J. J. Back,⁵⁵ S. Baker,⁶⁰ V. Balagura,^{11,b} W. Baldini,²⁰ J. Baptista Leite,¹ R. J. Barlow,⁶¹ S. Barsuk,¹¹ W. Barter,⁶⁰ M. Bartolini,^{23,47,h} F. Baryshnikov,⁷⁸ J. M. Basels,¹³ G. Bassi,²⁸ V. Batozskaya,³⁵ B. Batsukh,⁶⁷ A. Battig,¹⁴ A. Bay,⁴⁸ M. Becker,¹⁴ F. Bedeschi,²⁸ I. Bediaga,¹ A. Beiter,⁶⁷ V. Belavin,⁴¹ S. Belin,²⁶ V. Bellec,⁴⁸ K. Belous,⁴³ I. Belyaev,³⁸ G. Bencivenni,²² E. Ben-Haim,¹² S. Benson,³¹ A. Berezhniov,³⁹ R. Bernet,⁴⁹ D. Berninghoff,¹⁶ H. C. Bernstein,⁶⁷ C. Bertella,⁴⁷ E. Bertholet,¹² A. Bertolin,²⁷ C. Betancourt,⁴⁹ F. Betti,^{19,e} M. O. Bettler,⁵⁴ I. Bezshyiko,⁴⁹ S. Bhasin,⁵³ J. Bhom,³³ M. S. Bieker,¹⁴ S. Bifani,⁵² P. Billoir,¹² A. Bizzeti,^{21,i} M. Bjørn,⁶² M. P. Blago,⁴⁷ T. Blake,⁵⁵ F. Blanc,⁴⁸ S. Blusk,⁶⁷ D. Bobulska,⁵⁸ V. Bocci,³⁰ O. Boente Garcia,⁴⁵ T. Boettcher,⁶³ A. Boldyrev,⁷⁹ A. Bondar,^{42,w} N. Bondar,^{37,47} S. Borghi,⁶¹ M. Borisov,⁴¹ M. Borsato,¹⁶ J. T. Borsuk,³³ T. J. V. Bowcock,⁵⁹ A. Boyer,⁴⁷ C. Bozzi,²⁰ M. J. Bradley,⁶⁰ S. Braun,⁶⁵ A. Brea Rodriguez,⁴⁵ M. Brodski,⁴⁷ J. Brodzicka,³³ A. Brossa Gonzalo,⁵⁵ D. Brundu,²⁶ E. Buchanan,⁵³ A. Büchler-Germann,⁴⁹ A. Buonauro,⁴⁹ C. Burr,⁴⁷ A. Bursche,²⁶ A. Butkevich,⁴⁰ J. S. Butter,³¹ J. Buytaert,⁴⁷ W. Byczynski,⁴⁷ S. Cadeddu,²⁶ H. Cai,⁷² R. Calabrese,^{20,g} L. Calero Diaz,²² S. Cali,²² R. Calladine,⁵² M. Calvi,^{24,i}

M. Calvo Gomez,^{44,l} P. Camargo Magalhaes,⁵³ A. Camboni,^{44,l} P. Campana,²² D. H. Campora Perez,³¹
 A. F. Campoverde Quezada,⁵ L. Capriotti,^{19,e} A. Carbone,^{19,e} G. Carboni,²⁹ R. Cardinale,^{23,h} A. Cardini,²⁶ I. Carli,⁶
 P. Carniti,^{24,i} K. Carvalho Akiba,³¹ A. Casais Vidal,⁴⁵ G. Casse,⁵⁹ M. Cattaneo,⁴⁷ G. Cavallero,⁴⁷ S. Celani,⁴⁸ R. Cenci,^{28,o}
 J. Cerasoli,¹⁰ M. G. Chapman,⁵³ M. Charles,¹² Ph. Charpentier,⁴⁷ G. Chatzikonstantinidis,⁵² M. Chefdeville,⁸
 V. Chekalina,⁴¹ C. Chen,³ S. Chen,²⁶ A. Chernov,³³ S.-G. Chitic,⁴⁷ V. Chobanova,⁴⁵ S. Cholak,⁴⁸ M. Chruszcz,³³
 A. Chubykin,³⁷ V. Chulikov,³⁷ P. Ciambone,²² M. F. Cicala,⁵⁵ X. Cid Vidal,⁴⁵ G. Ciezarek,⁴⁷ F. Cindolo,¹⁹ P. E. L. Clarke,⁵⁷
 M. Clemencic,⁴⁷ H. V. Cliff,⁵⁴ J. Closier,⁴⁷ J. L. Cobbledick,⁶¹ V. Coco,⁴⁷ J. A. B. Coelho,¹¹ J. Cogan,¹⁰ E. Cogneras,⁹
 L. Cojocariu,³⁶ P. Collins,⁴⁷ T. Colombo,⁴⁷ A. Contu,²⁶ N. Cooke,⁵² G. Coombs,⁵⁸ S. Coquereau,⁴⁴ G. Corti,⁴⁷
 C. M. Costa Sobral,⁵⁵ B. Couturier,⁴⁷ D. C. Craik,⁶³ J. Crkovská,⁶⁶ A. Crocombe,⁵⁵ M. Cruz Torres,^{1,z} R. Currie,⁵⁷
 C. L. Da Silva,⁶⁶ E. Dall'Occo,¹⁴ J. Dalseno,^{45,53} C. D'Ambrosio,⁴⁷ A. Danilina,³⁸ P. d'Argent,⁴⁷ A. Davis,⁶¹
 O. De Aguiar Francisco,⁴⁷ K. De Bruyn,⁴⁷ S. De Capua,⁶¹ M. De Cian,⁴⁸ J. M. De Miranda,¹ L. De Paula,² M. De Serio,^{18,d}
 P. De Simone,²² J. A. de Vries,⁷⁶ C. T. Dean,⁶⁶ W. Dean,⁸¹ D. Decamp,⁸ L. Del Buono,¹² B. Delaney,⁵⁴ H.-P. Dembinski,¹⁴
 A. Dendek,³⁴ V. Denysenko,⁴⁹ D. Derkach,⁷⁹ O. Deschamps,⁹ F. Desse,¹¹ F. Dettori,^{26,f} B. Dey,⁷ A. Di Canto,⁴⁷
 P. Di Nezza,²² S. Didenko,⁷⁸ H. Dijkstra,⁴⁷ V. Dobishuk,⁵¹ F. Dordei,²⁶ M. Dorigo,^{28,x} A. C. dos Reis,¹ L. Douglas,⁵⁸
 A. Dovbnya,⁵⁰ K. Dreimanis,⁵⁹ M. W. Dudek,³³ L. Dufour,⁴⁷ P. Durante,⁴⁷ J. M. Durham,⁶⁶ D. Dutta,⁶¹ M. Dziewiecki,¹⁶
 A. Dziurda,³³ A. Dzyuba,³⁷ S. Easo,⁵⁶ U. Egede,⁶⁹ V. Egorychev,³⁸ S. Eidelman,^{42,w} S. Eisenhardt,⁵⁷ S. Ek-In,⁴⁸ L. Eklund,⁵⁸
 S. Ely,⁶⁷ A. Ene,³⁶ E. Epple,⁶⁶ S. Escher,¹³ J. Eschle,⁴⁹ S. Esen,³¹ T. Evans,⁴⁷ A. Falabella,¹⁹ J. Fan,³ Y. Fan,⁵ N. Farley,⁵²
 S. Farry,⁵⁹ D. Fazzini,¹¹ P. Fedin,³⁸ M. Féo,⁴⁷ P. Fernandez Declara,⁴⁷ A. Fernandez Prieto,⁴⁵ F. Ferrari,^{19,e}
 L. Ferreira Lopes,⁴⁸ F. Ferreira Rodrigues,² S. Ferreres Sole,³¹ M. Ferrillo,⁴⁹ M. Ferro-Luzzi,⁴⁷ S. Filippov,⁴⁰ R. A. Fini,¹⁸
 M. Fiorini,^{20,g} M. Firlej,³⁴ K. M. Fischer,⁶² C. Fitzpatrick,⁶¹ T. Fiutowski,³⁴ F. Fleuret,^{11,b} M. Fontana,⁴⁷ F. Fontanelli,^{23,h}
 R. Forty,⁴⁷ V. Franco Lima,⁵⁹ M. Franco Sevilla,⁶⁵ M. Frank,⁴⁷ C. Frei,⁴⁷ D. A. Friday,⁵⁸ J. Fu,^{25,p} Q. Fuehring,¹⁴ W. Funk,⁴⁷
 E. Gabriel,⁵⁷ T. Gaintseva,⁴¹ A. Gallas Torreira,⁴⁵ D. Galli,^{19,e} S. Gallorini,²⁷ S. Gambetta,⁵⁷ Y. Gan,³ M. Gandelman,²
 P. Gandini,²⁵ Y. Gao,⁴ L. M. Garcia Martin,⁴⁶ J. García Pardiñas,⁴⁹ B. Garcia Plana,⁴⁵ F. A. Garcia Rosales,¹¹ L. Garrido,⁴⁴
 D. Gascon,⁴⁴ C. Gaspar,⁴⁷ D. Gerick,¹⁶ E. Gersabeck,⁶¹ M. Gersabeck,⁶¹ T. Gershon,⁵⁵ D. Gerstel,¹⁰ Ph. Ghez,⁸ V. Gibson,⁵⁴
 A. Gioventù,⁴⁵ P. Gironella Gironell,⁴⁴ L. Giubega,³⁶ C. Giugliano,²⁰ K. Gizdov,⁵⁷ V. V. Gligorov,¹² C. Göbel,⁷⁰
 E. Golobardes,^{44,l} D. Golubkov,³⁸ A. Golutvin,^{60,78} A. Gomes,^{1,a} P. Gorbounov,³⁸ I. V. Gorelov,³⁹ C. Gotti,^{24,i}
 E. Govorkova,³¹ J. P. Grabowski,¹⁶ R. Graciani Diaz,⁴⁴ T. Grammatico,¹² L. A. Granado Cardoso,⁴⁷ E. Graugés,⁴⁴
 E. Graverini,⁴⁸ G. Graziani,²¹ A. Grecu,³⁶ R. Greim,³¹ P. Griffith,²⁰ L. Grillo,⁶¹ L. Gruber,⁴⁷ B. R. Gruber Cazon,⁶² C. Gu,³
 M. Guarise,²⁰ E. Gushchin,⁴⁰ A. Guth,¹³ Yu. Guz,^{43,47} T. Gys,⁴⁷ P. A. Günther,¹⁶ T. Hadavizadeh,⁶² G. Haefeli,⁴⁸ C. Haen,⁴⁷
 S. C. Haines,⁵⁴ P. M. Hamilton,⁶⁵ Q. Han,⁷ X. Han,¹⁶ T. H. Hancock,⁶² S. Hansmann-Menzemer,¹⁶ N. Harnew,⁶²
 T. Harrison,⁵⁹ R. Hart,³¹ C. Hasse,¹⁴ M. Hatch,⁴⁷ J. He,⁵ M. Hecker,⁶⁰ K. Heijhoff,³¹ K. Heinicke,¹⁴ A. M. Hennequin,⁴⁷
 K. Hennessy,⁵⁹ L. Henry,^{25,46} J. Heuel,¹³ A. Hicheur,⁶⁸ D. Hill,⁶² M. Hilton,⁶¹ P. H. Hopchev,⁴⁸ J. Hu,¹⁶ J. Hu,⁷¹ W. Hu,⁷
 W. Huang,⁵ W. Hulsbergen,³¹ T. Humair,⁶⁰ R. J. Hunter,⁵⁵ M. Hushchyn,⁷⁹ D. Hutchcroft,⁵⁹ D. Hynds,³¹ P. Ibis,¹⁴ M. Idzik,³⁴
 P. Ilten,⁵² A. Inglessi,³⁷ K. Ivshin,³⁷ R. Jacobsson,⁴⁷ S. Jakobsen,⁴⁷ E. Jans,³¹ B. K. Jashal,⁴⁶ A. Jawahery,⁶⁵ V. Jevtic,¹⁴
 F. Jiang,³ M. John,⁶² D. Johnson,⁴⁷ C. R. Jones,⁵⁴ B. Jost,⁴⁷ N. Jurik,⁶² S. Kandybei,⁵⁰ M. Karacson,⁴⁷ J. M. Kariuki,⁵³
 N. Kazeev,⁷⁹ M. Kecke,¹⁶ F. Keizer,^{54,47} M. Kelsey,⁶⁷ M. Kenzie,⁵⁵ T. Ketel,³² B. Khanji,⁴⁷ A. Kharisova,⁸⁰ K. E. Kim,⁶⁷
 T. Kim,¹³ V. S. Kirsebom,⁴⁸ S. Klaver,²² K. Klimaszewski,³⁵ S. Koliiiev,⁵¹ A. Kondybayeva,⁷⁸ A. Konoplyannikov,³⁸
 P. Kopciwicz,³⁴ R. Kopečna,¹⁶ P. Koppenburg,³¹ M. Korolev,³⁹ I. Kostiuik,^{31,51} O. Kot,⁵¹ S. Kotriakhova,³⁷ L. Kravchuk,⁴⁰
 R. D. Krawczyk,⁴⁷ M. Kreps,⁵⁵ F. Kress,⁶⁰ S. Kretzschmar,¹³ P. Krokovny,^{42,w} W. Krupa,³⁴ W. Krzemien,³⁵ W. Kucewicz,^{33,k}
 M. Kucharczyk,³³ V. Kudryavtsev,^{42,w} H. S. Kuindersma,³¹ G. J. Kunde,⁶⁶ T. Kvaratskheliya,³⁸ D. Lacarrere,⁴⁷ G. Lafferty,⁶¹
 A. Lai,²⁶ D. Lancierini,⁴⁹ J. J. Lane,⁶¹ G. Lanfranchi,²² C. Langenbruch,¹³ O. Lantwin,^{49,78} T. Latham,⁵⁵ F. Lazzari,^{28,u}
 R. Le Gac,¹⁰ S. H. Lee,⁸¹ R. Lefèvre,⁹ A. Leflat,^{39,47} O. Leroy,¹⁰ T. Lesiak,³³ B. Leverington,¹⁶ H. Li,⁷¹ L. Li,⁶² X. Li,⁶⁶
 Y. Li,⁶ Z. Li,⁶⁷ X. Liang,⁶⁷ T. Lin,⁶⁰ R. Lindner,⁴⁷ V. Lisovskyi,¹⁴ G. Liu,⁷¹ X. Liu,³ D. Loh,⁵⁵ A. Loi,²⁶ J. Lomba Castro,⁴⁵
 I. Longstaff,⁵⁸ J. H. Lopes,² G. Loustau,⁴⁹ G. H. Lovell,⁵⁴ Y. Lu,⁶ D. Lucchesi,^{27,n} M. Lucio Martinez,³¹ Y. Luo,³
 A. Lupato,⁶¹ E. Luppi,^{20,g} O. Lupton,⁵⁵ A. Lusiani,^{28,s} X. Lyu,⁵ S. Maccolini,^{19,e} F. Machefert,¹¹ F. Maciuc,³⁶ V. Macko,⁴⁸
 P. Mackowiak,¹⁴ S. Maddrell-Mander,⁵³ L. R. Madhan Mohan,⁵³ O. Maev,³⁷ A. Maevskiy,⁷⁹ D. Maisuzenko,³⁷
 M. W. Majewski,³⁴ S. Malde,⁶² B. Malecki,⁴⁷ A. Malinin,⁷⁷ T. Maltsev,^{42,w} H. Malygina,¹⁶ G. Manca,^{26,f} G. Mancinelli,¹⁰
 R. Manera Escalero,⁴⁴ D. Manuzzi,^{19,e} D. Marangotto,^{25,p} J. Maratas,^{9,v} J. F. Marchand,⁸ U. Marconi,¹⁹ S. Mariani,^{21,47,21}
 C. Marin Benito,¹¹ M. Marinangeli,⁴⁸ P. Marino,⁴⁸ J. Marks,¹⁶ P. J. Marshall,⁵⁹ G. Martellotti,³⁰ L. Martinazzoli,⁴⁷

M. Martinelli,^{24,i} D. Martinez Santos,⁴⁵ F. Martinez Vidal,⁴⁶ A. Massafferri,¹ M. Materok,¹³ R. Matev,⁴⁷ A. Mathad,⁴⁹
 Z. Mathe,⁴⁷ V. Matiunin,³⁸ C. Matteuzzi,²⁴ K. R. Mattioli,⁸¹ A. Mauri,⁴⁹ E. Maurice,^{11,b} M. McCann,⁶⁰ L. McConnell,¹⁷
 A. McNab,⁶¹ R. McNulty,¹⁷ J. V. Mead,⁵⁹ B. Meadows,⁶⁴ C. Meaux,¹⁰ G. Meier,¹⁴ N. Meinert,⁷⁴ D. Melnychuk,³⁵
 S. Meloni,^{24,i} M. Merk,³¹ A. Merli,²⁵ L. Meyer Garcia,² M. Mikhasenko,⁴⁷ D. A. Milanes,⁷³ E. Millard,⁵⁵ M.-N. Minard,⁸
 O. Mineev,³⁸ L. Minzoni,²⁰ S. E. Mitchell,⁵⁷ B. Mitreska,⁶¹ D. S. Mitzel,⁴⁷ A. Mödden,¹⁴ A. Mogini,¹² R. D. Moise,⁶⁰
 T. Mombächer,¹⁴ I. A. Monroy,⁷³ S. Monteil,⁹ M. Morandin,²⁷ G. Morello,²² M. J. Morello,^{28,s} J. Moron,³⁴ A. B. Morris,¹⁰
 A. G. Morris,⁵⁵ R. Mountain,⁶⁷ H. Mu,³ F. Muheim,⁵⁷ M. Mukherjee,⁷ M. Mulder,⁴⁷ D. Müller,⁴⁷ K. Müller,⁴⁹
 C. H. Murphy,⁶² D. Murray,⁶¹ P. Muzzetto,²⁶ P. Naik,⁵³ T. Nakada,⁴⁸ R. Nandakumar,⁵⁶ T. Nanut,⁴⁸ I. Nasteva,²
 M. Needham,⁵⁷ I. Neri,²⁰ N. Neri,^{25,p} S. Neubert,¹⁶ N. Neufeld,⁴⁷ R. Newcombe,⁶⁰ T. D. Nguyen,⁴⁸ C. Nguyen-Mau,^{48,m}
 E. M. Niel,¹¹ S. Nieswand,¹³ N. Nikitin,³⁹ N. S. Nolte,⁴⁷ C. Nunez,⁸¹ A. Oblakowska-Mucha,³⁴ V. Obraztsov,⁴³ S. Ogilvy,⁵⁸
 D. P. O'Hanlon,⁵³ R. Oldeman,^{26,f} C. J. G. Onderwater,⁷⁵ J. D. Osborn,⁸¹ A. Ossowska,³³ J. M. Otalora Goicochea,²
 T. Ovsiannikova,³⁸ P. Owen,⁴⁹ A. Oyanguren,⁴⁶ P. R. Pais,⁴⁸ T. Pajero,^{28,47,28,s} A. Palano,¹⁸ M. Palutan,²² G. Panshin,⁸⁰
 A. Papanestis,⁵⁶ M. Pappagallo,⁵⁷ L. L. Pappalardo,²⁰ C. Pappenheimer,⁶⁴ W. Parker,⁶⁵ C. Parkes,⁶¹ C. J. Parkinson,⁴⁵
 G. Passaleva,^{21,47} A. Pastore,¹⁸ M. Patel,⁶⁰ C. Patrignani,^{19,e} A. Pearce,⁴⁷ A. Pellegrino,³¹ M. Pepe Altarelli,⁴⁷ S. Perazzini,¹⁹
 D. Pereima,³⁸ P. Perret,⁹ K. Petridis,⁵³ A. Petrolini,^{23,h} A. Petrov,⁷⁷ S. Petrucci,⁵⁷ M. Petruzzio,^{25,p} B. Pietrzyk,⁸ G. Pietrzyk,⁴⁸
 M. Pili,⁶² D. Pinci,³⁰ J. Pinzino,⁴⁷ F. Pisani,¹⁹ A. Piucci,¹⁶ V. Placinta,³⁶ S. Playfer,⁵⁷ J. Plews,⁵² M. Plo Casasus,⁴⁵ F. Polci,¹²
 M. Poli Lener,²² M. Poliakov,⁶⁷ A. Poluektov,¹⁰ N. Polukhina,^{78,c} I. Polyakov,⁶⁷ E. Polycarpo,² G. J. Pomery,⁵³ S. Ponce,⁴⁷
 A. Popov,⁴³ D. Popov,⁵² S. Poslavskii,⁴³ K. Prasanth,³³ L. Promberger,⁴⁷ C. Prouve,⁴⁵ V. Pugatch,⁵¹ A. Puig Navarro,⁴⁹
 H. Pullen,⁶² G. Punzi,^{28,o} W. Qian,⁵ J. Qin,⁵ R. Quagliani,¹² B. Quintana,⁸ N. V. Raab,¹⁷ R. I. Rabadan Trejo,¹⁰ B. Rachwal,³⁴
 J. H. Rademacker,⁵³ M. Rama,²⁸ M. Ramos Pernas,⁴⁵ M. S. Rangel,² F. Ratnikov,^{41,79} G. Raven,³² M. Reboud,⁸ F. Redi,⁴⁸
 F. Reiss,¹² C. Remon Alepuz,⁴⁶ Z. Ren,³ V. Renaudin,⁶² S. Ricciardi,⁵⁶ D. S. Richards,⁵⁶ S. Richards,⁵³ K. Rinnert,⁵⁹
 P. Robbe,¹¹ A. Robert,¹² A. B. Rodrigues,⁴⁸ E. Rodrigues,⁵⁹ J. A. Rodriguez Lopez,⁷³ M. Roehrken,⁴⁷ A. Rollings,⁶²
 V. Romanovskiy,⁴³ M. Romero Lamas,⁴⁵ A. Romero Vidal,⁴⁵ J. D. Roth,⁸¹ M. Rotondo,²² M. S. Rudolph,⁶⁷ T. Ruf,⁴⁷
 J. Ruiz Vidal,⁴⁶ A. Ryzhikov,⁷⁹ J. Ryzka,³⁴ J. J. Saborido Silva,⁴⁵ N. Sagidova,³⁷ N. Sahoo,⁵⁵ B. Saitta,^{26,f} C. Sanchez Gras,³¹
 C. Sanchez Mayordomo,⁴⁶ R. Santacesaria,³⁰ C. Santamarina Rios,⁴⁵ M. Santimaria,²² E. Santovetti,^{29,j} G. Sarpis,⁶¹
 M. Sarpis,¹⁶ A. Sarti,³⁰ C. Satriano,^{30,r} A. Satta,²⁹ M. Saur,⁵ D. Savrina,^{38,39} L. G. Scantlebury Smead,⁶² S. Schael,¹³
 M. Schellenberg,¹⁴ M. Schiller,⁵⁸ H. Schindler,⁴⁷ M. Schmelling,¹⁵ T. Schmelzer,¹⁴ B. Schmidt,⁴⁷ O. Schneider,⁴⁸
 A. Schopper,⁴⁷ H. F. Schreiner,⁶⁴ M. Schubiger,³¹ S. Schulte,⁴⁸ M. H. Schune,¹¹ R. Schwemmer,⁴⁷ B. Sciascia,²²
 A. Sciubba,²² S. Sellam,⁶⁸ A. Semennikov,³⁸ A. Sergi,^{52,47} N. Serra,⁴⁹ J. Serrano,¹⁰ L. Sestini,²⁷ A. Seuthe,¹⁴ P. Seyfert,⁴⁷
 D. M. Shangase,⁸¹ M. Shapkin,⁴³ L. Shchutska,⁴⁸ T. Shears,⁵⁹ L. Shekhtman,^{42,w} V. Shevchenko,⁷⁷ E. Shmanin,⁷⁸
 J. D. Shupperd,⁶⁷ B. G. Siddi,²⁰ R. Silva Coutinho,⁴⁹ L. Silva de Oliveira,² G. Simi,^{27,n} S. Simone,^{18,d} I. Skiba,²⁰
 N. Skidmore,¹⁶ T. Skwarnicki,⁶⁷ M. W. Slater,⁵² J. G. Smeaton,⁵⁴ A. Smetkina,³⁸ E. Smith,¹³ I. T. Smith,⁵⁷ M. Smith,⁶⁰
 A. Snoch,³¹ M. Soares,¹⁹ L. Soares Lavra,⁹ M. D. Sokoloff,⁶⁴ F. J. P. Soler,⁵⁸ B. Souza De Paula,² B. Spaan,¹⁴
 E. Spadaro Norella,^{25,p} P. Spradlin,⁵⁸ F. Stagni,⁴⁷ M. Stahl,⁶⁴ S. Stahl,⁴⁷ P. Stefko,⁴⁸ O. Steinkamp,^{49,78} S. Stemmler,¹⁶
 O. Stenyakin,⁴³ M. Stepanova,³⁷ H. Stevens,¹⁴ S. Stone,⁶⁷ S. Stracka,²⁸ M. E. Stramaglia,⁴⁸ M. Straticiu,³⁶ S. Strov,⁸⁰
 J. Sun,²⁶ L. Sun,⁷² Y. Sun,⁶⁵ P. Sviha,⁶¹ K. Swientek,³⁴ A. Szabelski,³⁵ T. Szumlak,³⁴ M. Szymanski,⁴⁷ S. Taneja,⁶¹ Z. Tang,³
 T. Tekampe,¹⁴ F. Teubert,⁴⁷ E. Thomas,⁴⁷ K. A. Thomson,⁵⁹ M. J. Tilley,⁶⁰ V. Tisserand,⁹ S. T'Jampens,⁸ M. Tobin,⁶
 S. Tolk,⁴⁷ L. Tomassetti,^{20,g} D. Torres Machado,¹ D. Y. Tou,¹² E. Tournefier,⁸ M. Traill,⁵⁸ M. T. Tran,⁴⁸ E. Trifonova,⁷⁸
 C. Trippel,⁴⁸ A. Tsaregorodtsev,¹⁰ G. Tuci,^{28,o} A. Tully,⁴⁸ N. Tuning,³¹ A. Ukleja,³⁵ A. Usachov,³¹ A. Ustyuzhanin,^{41,79}
 U. Uwer,¹⁶ A. Vagner,⁸⁰ V. Vagnoni,¹⁹ A. Valassi,⁴⁷ G. Valenti,¹⁹ M. van Beuzekom,³¹ H. Van Hecke,⁶⁶ E. van Herwijnen,⁴⁷
 C. B. Van Hulse,¹⁷ M. van Veghel,⁷⁵ R. Vazquez Gomez,⁴⁴ P. Vazquez Regueiro,⁴⁵ C. Vázquez Sierra,³¹ S. Vecchi,²⁰
 J. J. Velthuis,⁵³ M. Veltri,^{21,q} A. Venkateswaran,⁶⁷ M. Veronesi,³¹ M. Vesterinen,⁵⁵ J. V. Viana Barbosa,⁴⁷ D. Vieira,⁶⁴
 M. Vieites Diaz,⁴⁸ H. Viemann,⁷⁴ X. Vilasis-Cardona,^{44,1} G. Vitali,²⁸ A. Vitkovskiy,³¹ A. Vollhardt,⁴⁹ D. Vom Bruch,¹²
 A. Vorobyev,³⁷ V. Vorobyev,^{42,w} N. Voropaev,³⁷ R. Waldi,⁷⁴ J. Walsh,²⁸ J. Wang,³ J. Wang,⁷² J. Wang,⁶ M. Wang,³ Y. Wang,⁷
 Z. Wang,⁴⁹ D. R. Ward,⁵⁴ H. M. Wark,⁵⁹ N. K. Watson,⁵² D. Websdale,⁶⁰ A. Weiden,⁴⁹ C. Weisser,⁶³ B. D. C. Westhenry,⁵³
 D. J. White,⁶¹ M. Whitehead,⁵³ D. Wiedner,¹⁴ G. Wilkinson,⁶² M. Wilkinson,⁶⁷ I. Williams,⁵⁴ M. Williams,⁶³
 M. R. J. Williams,⁶¹ T. Williams,⁵² F. F. Wilson,⁵⁶ W. Wislicki,³⁵ M. Witek,³³ L. Witola,¹⁶ G. Wormser,¹¹ S. A. Wotton,⁵⁴
 H. Wu,⁶⁷ K. Wyllie,⁴⁷ Z. Xiang,⁵ D. Xiao,⁷ Y. Xie,⁷¹ H. Xing,⁷¹ A. Xu,⁴ J. Xu,⁵ L. Xu,³ M. Xu,⁷ Q. Xu,⁵ Z. Xu,⁴ Z. Xu,⁵
 Z. Yang,³ Z. Yang,⁶⁵ Y. Yao,⁶⁷ L. E. Yeomans,⁵⁹ H. Yin,⁷ J. Yu,⁷ X. Yuan,⁶⁷ O. Yushchenko,⁴³ K. A. Zarebski,⁵²

M. Zavertyaev,^{15,c} M. Zdybal,³³ M. Zeng,³ D. Zhang,⁷ L. Zhang,³ S. Zhang,⁴ W. C. Zhang,^{3,y} Y. Zhang,⁴⁷ A. Zhelezov,¹⁶
Y. Zheng,⁵ X. Zhou,⁵ Y. Zhou,⁵ X. Zhu,³ V. Zhukov,^{13,39} J. B. Zonneveld,⁵⁷ and S. Zucchelli^{19,e}

(LHCb Collaboration)

¹*Centro Brasileiro de Pesquisas Físicas (CBPF), Rio de Janeiro, Brazil*

²*Universidade Federal do Rio de Janeiro (UFRJ), Rio de Janeiro, Brazil*

³*Center for High Energy Physics, Tsinghua University, Beijing, China*

⁴*School of Physics State Key Laboratory of Nuclear Physics and Technology, Peking University, Beijing, China*

⁵*University of Chinese Academy of Sciences, Beijing, China*

⁶*Institute of High Energy Physics (IHEP), Beijing, China*

⁷*Institute of Particle Physics, Central China Normal University, Wuhan, Hubei, China*

⁸*Université Grenoble Alpes, Université Savoie Mont Blanc, CNRS, IN2P3-LAPP, Annecy, France*

⁹*Université Clermont Auvergne, CNRS/IN2P3, LPC, Clermont-Ferrand, France*

¹⁰*Aix Marseille Université, CNRS/IN2P3, CPPM, Marseille, France*

¹¹*Université Paris-Saclay, CNRS/IN2P3, IJCLab, Orsay, France*

¹²*LPNHE, Sorbonne Université, Paris Diderot Sorbonne Paris Cité, CNRS/IN2P3, Paris, France*

¹³*I. Physikalisches Institut, RWTH Aachen University, Aachen, Germany*

¹⁴*Fakultät Physik, Technische Universität Dortmund, Dortmund, Germany*

¹⁵*Max-Planck-Institut für Kernphysik (MPIK), Heidelberg, Germany*

¹⁶*Physikalisches Institut, Ruprecht-Karls-Universität Heidelberg, Heidelberg, Germany*

¹⁷*School of Physics, University College Dublin, Dublin, Ireland*

¹⁸*INFN Sezione di Bari, Bari, Italy*

¹⁹*INFN Sezione di Bologna, Bologna, Italy*

²⁰*INFN Sezione di Ferrara, Ferrara, Italy*

²¹*INFN Sezione di Firenze, Firenze, Italy*

²²*INFN Laboratori Nazionali di Frascati, Frascati, Italy*

²³*INFN Sezione di Genova, Genova, Italy*

²⁴*INFN Sezione di Milano-Bicocca, Milano, Italy*

²⁵*INFN Sezione di Milano, Milano, Italy*

²⁶*INFN Sezione di Cagliari, Monserrato, Italy*

²⁷*INFN Sezione di Padova, Padova, Italy*

²⁸*INFN Sezione di Pisa, Pisa, Italy*

²⁹*INFN Sezione di Roma Tor Vergata, Roma, Italy*

³⁰*INFN Sezione di Roma La Sapienza, Roma, Italy*

³¹*Nikhef National Institute for Subatomic Physics, Amsterdam, Netherlands*

³²*Nikhef National Institute for Subatomic Physics and VU University Amsterdam, Amsterdam, Netherlands*

³³*Henryk Niewodniczanski Institute of Nuclear Physics Polish Academy of Sciences, Kraków, Poland*

³⁴*AGH—University of Science and Technology, Faculty of Physics and Applied Computer Science, Kraków, Poland*

³⁵*National Center for Nuclear Research (NCBJ), Warsaw, Poland*

³⁶*Horia Hulubei National Institute of Physics and Nuclear Engineering, Bucharest-Magurele, Romania*

³⁷*Petersburg Nuclear Physics Institute NRC Kurchatov Institute (PNPI NRC KI), Gatchina, Russia*

³⁸*Institute of Theoretical and Experimental Physics NRC Kurchatov Institute (ITEP NRC KI), Moscow, Russia*

³⁹*Institute of Nuclear Physics, Moscow State University (SINP MSU), Moscow, Russia*

⁴⁰*Institute for Nuclear Research of the Russian Academy of Sciences (INR RAS), Moscow, Russia*

⁴¹*Yandex School of Data Analysis, Moscow, Russia*

⁴²*Budker Institute of Nuclear Physics (SB RAS), Novosibirsk, Russia*

⁴³*Institute for High Energy Physics NRC Kurchatov Institute (IHEP NRC KI), Protvino, Russia, Protvino, Russia*

⁴⁴*ICCUB, Universitat de Barcelona, Barcelona, Spain*

⁴⁵*Instituto Galego de Física de Altas Enerxías (IGFAE), Universidade de Santiago de Compostela, Santiago de Compostela, Spain*

⁴⁶*Instituto de Física Corpuscular, Centro Mixto Universidad de Valencia—CSIC, Valencia, Spain*

⁴⁷*European Organization for Nuclear Research (CERN), Geneva, Switzerland*

⁴⁸*Institute of Physics, Ecole Polytechnique Fédérale de Lausanne (EPFL), Lausanne, Switzerland*

⁴⁹*Physik-Institut, Universität Zürich, Zürich, Switzerland*

⁵⁰*NSC Kharkiv Institute of Physics and Technology (NSC KIPT), Kharkiv, Ukraine*

⁵¹*Institute for Nuclear Research of the National Academy of Sciences (KINR), Kyiv, Ukraine*

⁵²*University of Birmingham, Birmingham, United Kingdom*

⁵³*H. H. Wills Physics Laboratory, University of Bristol, Bristol, United Kingdom*

- ⁵⁴*Cavendish Laboratory, University of Cambridge, Cambridge, United Kingdom*
- ⁵⁵*Department of Physics, University of Warwick, Coventry, United Kingdom*
- ⁵⁶*STFC Rutherford Appleton Laboratory, Didcot, United Kingdom*
- ⁵⁷*School of Physics and Astronomy, University of Edinburgh, Edinburgh, United Kingdom*
- ⁵⁸*School of Physics and Astronomy, University of Glasgow, Glasgow, United Kingdom*
- ⁵⁹*Oliver Lodge Laboratory, University of Liverpool, Liverpool, United Kingdom*
- ⁶⁰*Imperial College London, London, United Kingdom*
- ⁶¹*Department of Physics and Astronomy, University of Manchester, Manchester, United Kingdom*
- ⁶²*Department of Physics, University of Oxford, Oxford, United Kingdom*
- ⁶³*Massachusetts Institute of Technology, Cambridge, Massachusetts, USA*
- ⁶⁴*University of Cincinnati, Cincinnati, Ohio, USA*
- ⁶⁵*University of Maryland, College Park, Maryland, USA*
- ⁶⁶*Los Alamos National Laboratory (LANL), Los Alamos, New Mexico, USA*
- ⁶⁷*Syracuse University, Syracuse, New York, USA*
- ⁶⁸*Laboratory of Mathematical and Subatomic Physics, Constantine, Algeria*
[associated with Universidade Federal do Rio de Janeiro (UFRJ), Rio de Janeiro, Brazil]
- ⁶⁹*School of Physics and Astronomy, Monash University, Melbourne, Australia*
(associated with Department of Physics, University of Warwick, Coventry, United Kingdom)
- ⁷⁰*Pontifícia Universidade Católica do Rio de Janeiro (PUC-Rio), Rio de Janeiro, Brazil*
[associated with Universidade Federal do Rio de Janeiro (UFRJ), Rio de Janeiro, Brazil]
- ⁷¹*Guangdong Provincial Key Laboratory of Nuclear Science, Institute of Quantum Matter, South China Normal University, Guangzhou, China*
(associated with Center for High Energy Physics, Tsinghua University, Beijing, China)
- ⁷²*School of Physics and Technology, Wuhan University, Wuhan, China*
(associated with Center for High Energy Physics, Tsinghua University, Beijing, China)
- ⁷³*Departamento de Física, Universidad Nacional de Colombia, Bogota, Colombia*
(associated with LPNHE, Sorbonne Université, Paris Diderot Sorbonne Paris Cité, CNRS/IN2P3, Paris, France)
- ⁷⁴*Institut für Physik, Universität Rostock, Rostock, Germany*
(associated with Physikalisches Institut, Ruprecht-Karls-Universität Heidelberg, Heidelberg, Germany)
- ⁷⁵*Van Swinderen Institute, University of Groningen, Groningen, Netherlands*
(associated with Nikhef National Institute for Subatomic Physics, Amsterdam, Netherlands)
- ⁷⁶*Universiteit Maastricht, Maastricht, Netherlands*
(associated with Nikhef National Institute for Subatomic Physics, Amsterdam, Netherlands)
- ⁷⁷*National Research Centre Kurchatov Institute, Moscow, Russia*
[associated with Institute of Theoretical and Experimental Physics NRC Kurchatov Institute (ITEP NRC KI), Moscow, Russia]
- ⁷⁸*National University of Science and Technology “MISIS,” Moscow, Russia*
[associated with Institute of Theoretical and Experimental Physics NRC Kurchatov Institute (ITEP NRC KI), Moscow, Russia]
- ⁷⁹*National Research University Higher School of Economics, Moscow, Russia*
(associated with Yandex School of Data Analysis, Moscow, Russia)
- ⁸⁰*National Research Tomsk Polytechnic University, Tomsk, Russia*
[associated with Institute of Theoretical and Experimental Physics NRC Kurchatov Institute (ITEP NRC KI), Moscow, Russia]
- ⁸¹*University of Michigan, Ann Arbor, Michigan, USA*
(associated with Syracuse University, Syracuse, New York, USA)
- ^aAlso at Universidade Federal do Triângulo Mineiro (UFTM), Uberaba-MG, Brazil.
- ^bAlso at Laboratoire Leprince-Ringuet, Palaiseau, France.
- ^cAlso at P.N. Lebedev Physical Institute, Russian Academy of Science (LPI RAS), Moscow, Russia.
- ^dAlso at Università di Bari, Bari, Italy.
- ^eAlso at Università di Bologna, Bologna, Italy.
- ^fAlso at Università di Cagliari, Cagliari, Italy.
- ^gAlso at Università di Ferrara, Ferrara, Italy.
- ^hAlso at Università di Genova, Genova, Italy.
- ⁱAlso at Università di Milano Bicocca, Milano, Italy.
- ^jAlso at Università di Roma Tor Vergata, Roma, Italy.
- ^kAlso at AGH—University of Science and Technology, Faculty of Computer Science, Electronics and Telecommunications, Kraków, Poland.
- ^lAlso at DS4DS, La Salle, Universitat Ramon Llull, Barcelona, Spain.
- ^mAlso at Hanoi University of Science, Hanoi, Vietnam.
- ⁿAlso at Università di Padova, Padova, Italy.
- ^oAlso at Università di Pisa, Pisa, Italy.

^pAlso at Università degli Studi di Milano, Milano, Italy.

^qAlso at Università di Urbino, Urbino, Italy.

^rAlso at Università della Basilicata, Potenza, Italy.

^sAlso at Scuola Normale Superiore, Pisa, Italy.

^tAlso at Università di Modena e Reggio Emilia, Modena, Italy.

^uAlso at Università di Siena, Siena, Italy.

^vAlso at MSU—Iligan Institute of Technology (MSU-IIT), Iligan, Philippines.

^wAlso at Novosibirsk State University, Novosibirsk, Russia.

^xAlso at INFN Sezione di Trieste, Trieste, Italy.

^yAlso at School of Physics and Information Technology, Shaanxi Normal University (SNNU), Xi'an, China.

^zAlso at Universidad Nacional Autonoma de Honduras, Tegucigalpa, Honduras.